The Journal of Eukaryotic Microbiology

ISOP Published by the International Society of Protistologists

Journal of Eukaryotic Microbiology ISSN 1066-5234

ORIGINAL ARTICLE

Kinesin-14 is Important for Chromosome Segregation During Mitosis and Meiosis in the Ciliate *Tetrahymena thermophila*

Yasuharu Kushida[a,b], Masak Takaine[a,c], Kentaro Nakano[a], Toshiro Sugai[a], Krishna Kumar Vasudevan[d], Mayukh Guha[d], Yu-Yang Jiang[d], Jacek Gaertig[d] & Osamu Numata[a]

a Graduate School of Life and Environmental Sciences, University of Tsukuba, Tsukuba, Ibaraki 305-8572, Japan
b Institute for Molecular and Cellular Regulation, Gunma University, Maebashi, Gunma 371-8512, Japan
c Gunma University Initiative for Advanced Research, Gunma University, Maebashi, Gunma 371-8511, Japan
d Department of Cellular Biology, University of Georgia, Athens, Georgia 30602, USA

Keywords
Macronucleus; micronucleus; microtubule; minus-end motors; spindle.

Correspondence
O. Numata, Graduate School of Life and Environmental Sciences, University of Tsukuba, 1-1-1 Tennodai, Tsukuba, Ibaraki 305-8572, Japan
Telephone/FAX number: +81-29-853-6648;
e-mail: numata.osamu.gb@u.tsukuba.ac.jp

Received: 5 July 2016; revised 26 August 2016; accepted August 30, 2016.
Early View publication September 23, 2016

doi:10.1111/jeu.12366

ABSTRACT

Ciliates such as *Tetrahymena thermophila* have two distinct nuclei within one cell: the micronucleus that undergoes mitosis and meiosis and the macronucleus that undergoes amitosis, a type of nuclear division that does not involve a bipolar spindle, but still relies on intranuclear microtubules. Ciliates provide an opportunity for the discovery of factors that specifically contribute to chromosome segregation based on a bipolar spindle, by identification of factors that affect the micronuclear but not the macronuclear division. Kinesin-14 is a conserved minus-end directed microtubule motor that cross-links microtubules and contributes to the bipolar spindle sizing and organization. Here, we use homologous DNA recombination to knock out genes that encode kinesin-14 orthologues (*KIN141*, *KIN142*) in *Tetrahymena*. A loss of KIN141 led to severe defects in the chromosome segregation during both mitosis and meiosis but did not affect amitosis. A loss of KIN141 altered the shape of the meiotic spindle in a way consistent with the KIN141's contribution to the organization of the spindle poles. EGFP-tagged KIN141 preferentially accumulated at the spindle poles during the meiotic prophase and metaphase I. Thus, in ciliates, kinesin-14 is important for nuclear divisions that involve a bipolar spindle.

CILIATES have two functionally distinct nuclei in the same cell (reviewed by Raikov 1982). The germline micronucleus (MIC) is a diploid nucleus that contains the entire genome that is transcriptionally silent, while the macronucleus (MAC) is a somatic polycopy nucleus that contains an expressed genome (reviewed in Cole and Sugai 2012). During the sexual phase, conjugation, the MIC undergoes meiosis, the gametic MICs are exchanged between partner cells and fuse to form zygotic MICs (Orias et al. 1983). A new set of MICs and MACs develops from the products of divisions of the zygotic MICs, and the parental MACs undergo programmed nuclear death (Akematsu et al. 2010). During the vegetative stage of the life cycle, the MIC chromosomes are segregated by a closed mitosis (Davidson and LaFountain 1975). The MAC contains thousands of mini-chromosomes (see Endo and Sugai 2011 and references therein) as a result of fragmentation of MIC-derived chromosomes that occurs when the new MAC develops from a zygotic MIC during conjugation (reviewed in Allen and Gibson 1972; Karrer 2012). During the vegetative multiplication, the MAC mini-chromosomes are segregated to daughter MACs by a simplified mode of nuclear division called amitosis (Nanney 1964), during which chromosomes do not condense and intranuclear microtubules are not organized into a bipolar spindle (Orias and Flacks 1975).

All types of nuclear divisions in ciliates, including mitosis, amitosis, and meiosis, depend on microtubules (MTs) (Kaczanowski et al. 1985; Tamura et al. 1969; Wunderlich and Peyk 1969; Wunderlich and Speth 1970). Intranuclear MTs associated with nuclear divisions in ciliates have been documented by electron microscopy (Davidson and LaFountain 1975; LaFountain and Davidson 1979, 1980; Wolfe et al. 1976) and immunofluorescence (Gaertig and Fleury 1992). In ciliates, all nuclear divisions proceed without a nuclear envelope break down (Jaeckel-Williams

1978). During nuclear divisions, MTs are polymerized inside the nucleoplasm especially in proximity to the nuclear envelope, which are called "peripheral sheath MTs (psMTs)" (Davidson and LaFountain 1975; LaFountain and Davidson 1979, 1980; Suganuma and Yamamoto 1992). Mitotic MIC contains other two classes of MTs, namely kinetochore MTs and non-kinetochore MTs. Although none of three classes of MTs span the full length of mitotic spindle, they form the bundle of MTs by overlapping each other, and support the shape of spindle (Davidson and LaFountain 1975; Gaertig and Fleury 1992; LaFountain and Davidson 1979, 1980). In addition, during the meiotic prophase, the MIC assumes a characteristic "crescent" shape at the time when the pairing of homologous chromosomes takes place (Kaczanowski et al. 1985; Loidl and Mochizuki 2009; Loidl and Scherthan 2004; Loidl et al. 2012; Mochizuki et al. 2008; Ray 1956) and the crescent formation is associated with bundles of MTs (Davidson and LaFountain 1975; Wolfe et al. 1976). During amitosis, scattered short MTs appear and rearrange into long bundles during the time when the MAC elongates and divides (Fujiu and Numata 2000; Ito et al. 1968; Kushida et al. 2011; Williams and Williams 1976). The presence of MT bundles during ciliate nuclear divisions indicates an involvement of MT-cross-linkers such as kinesin and dynein motors, which in other species are known to organize both parallel and antiparallel aligned MTs (reviewed in Cross and McAinsh 2014). A cytoplasmic dynein, Dyh1p, contributes to the accuracy of mitotic chromosome segregation in *Tetrahymena* (Lee et al. 1999), and at present is the only known potential MT-cross-linker identified during mitosis of ciliates.

Kinesin-14 homologs have a C-terminal minus-end-directed motor domain (Chandra et al. 1993; McDonald et al. 1990; Pechatnikova and Taylor 1997, 1999) and an N-terminal non-motor MT-binding domain (Karabay and Walker 1999, 2003). Due to the presence of two MT-interacting domains, kinesin-14 can cross-link parallel spindle MTs (Mountain et al. 1999) and align them into spindle poles (Hatsumi and Endow 1992; Kim and Song 2013). Kinesin-14 contributes to the proper segregation of chromosomes (Endow et al. 1990; Winey and Bloom 2012). Here, we address the function of two kinesin-14 orthologues, *KIN141* and *KIN142* in *Tetrahymena thermophila*.

MATERIALS AND METHODS

Phylogenetic analysis

Sequences encoding *T. thermophila* kinesin-14 were searched for in the *Tetrahymena* MAC genome database (TGD: http://ciliate.org/index.php/home/welcome), and

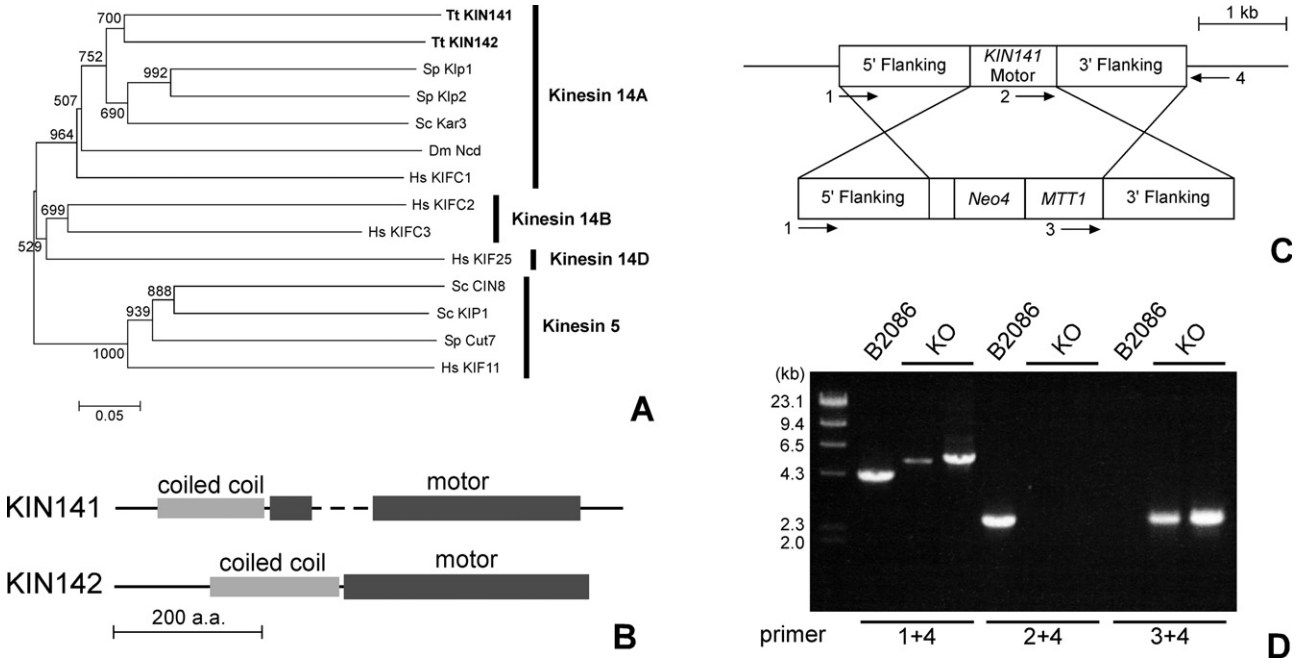

Figure 1 KO strategies for the *Tetrahymena* kinesin-14s genes: *KIN141* and *KIN142*. (**A**) A phylogenic analysis of kinesin-14 homologs of *Tetrahymena* together with human, yeasts, and fruit fly homologs. *KIN141* and *KIN142* (bold letters) cluster with the "kinesin-14A" subgroup, containing known mitotic and meiotic minus-end-directed kinesin-14 motors. Tt, *Tetrahymena thermophila*; Sp, *Schizosaccharomyces pombe*; Sc, *Saccharomyces cerevisiae*; Hs, *Homo sapiens*; Dm, *Drosophila melanogaster*. Bootstrap values indicate common branching order confidence out of 1,000 trials. The bar indicates 0.05 amino acid replacement. (**B**) Predicted protein domain organizations of the *Tetrahymena* kinesin-14s. (**C**) Strategies for knockouts gene segments encoding the motor domain of KIN141 using DNA homologous recombination. See Supporting Information (Fig. S1) for the gene KO constructs for targeting of *KIN142*. Arrows indicate primers used for check PCR in panel D. (**D**) A PCR that confirms a gene KO has occurred in *KIN141*. Genomic DNA was extracted from the wild-type strain B2086 and two separate *KIN141*-KO strains and processed for PCR. Numbers below the gel image indicate primers sets whose positions are marked in C.

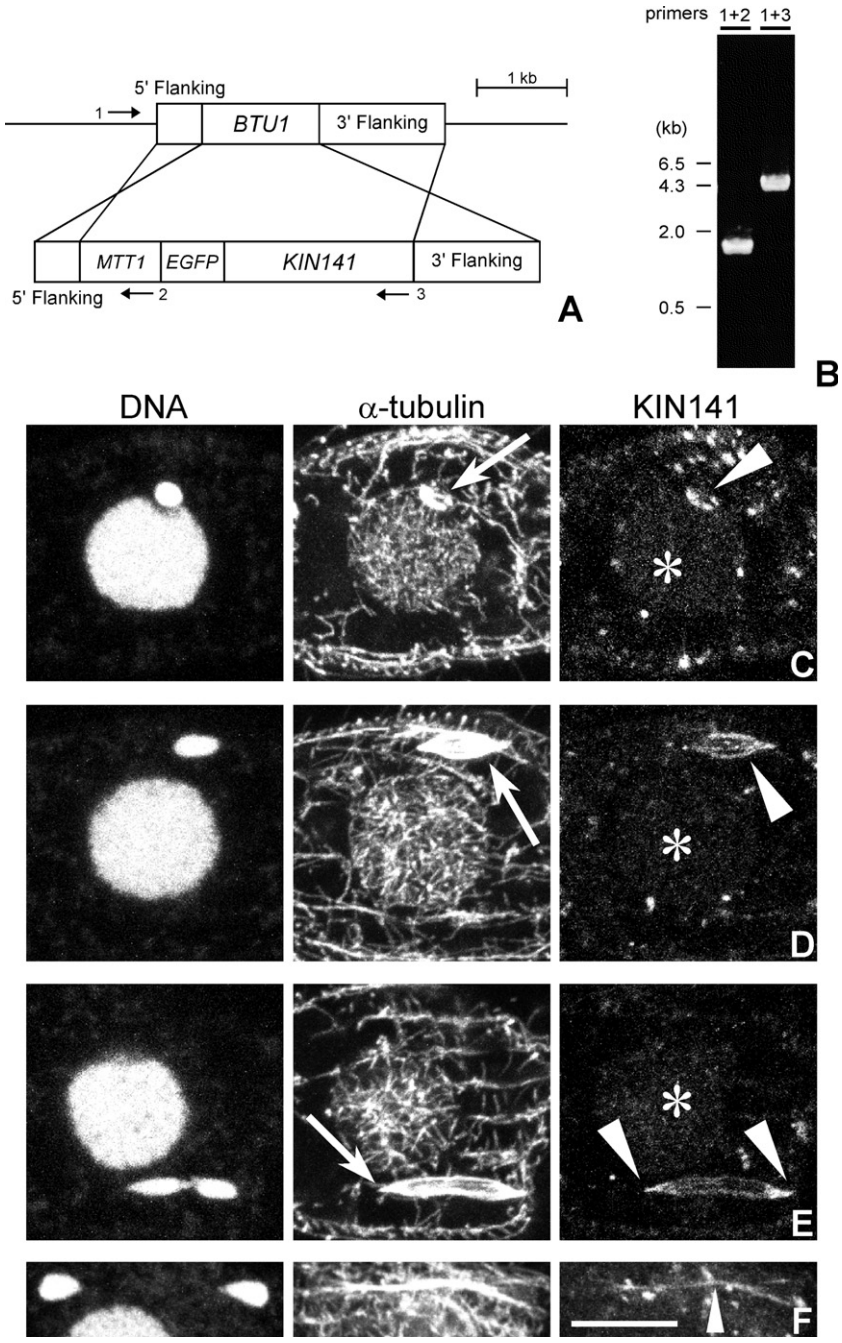

Figure 2 Localization of EGFP-KIN141 during mitosis. (**A**) A strategy for overexpression of EGFP-KIN141 using DNA homologous recombination. A mutated *BTU1* coding region of the strain CU522 was replaced by biolistic transformation and taxol selection as described in Gaertig et al. (1999). (**B**) A PCR test confirms the intended transgene insertion. Numbers on top of each lane indicate primer sets whose positions are marked in A. (**C–F**) Immunofluorescence images for anti-α-tubulin and anti-GFP antibodies. DNA is stained with DAPI. Asterisks indicate the MAC during early amitosis. (C) Early mitotic prophase. Arrow indicates the MIC MTs. KIN141 localized along the MIC MTs (arrowhead). (D) Mitotic prophase. The mitotic spindle is present inside the MIC (arrow). KIN141 localized uniformly along the spindle MTs (arrowhead). (E) Early mitotic anaphase. The arrow indicates a mitotic anaphase spindle in the MIC. Most of the KIN141 signal is present at the both ends of the mitotic spindle (arrowheads). (F) Late mitotic anaphase. KIN141 localizes to the MT bundles in the dumbbell-shaped MICs (Arrowhead). Scale bar: 10 μm.

their motor domains were identified by the NCBI Protein BLAST (http://blast.ncbi.nlm.nih.gov/) or SMART programs (http://smart.embl-heidelberg.de/). A multiple protein sequence alignment was carried out by "BioEdit" (version 7.0.5.3; http://www.mbio.ncsu.edu/bioedit/bioedit.html), and an amino acid sequence of the well-conserved region of the motor domain (from the 3rd to the 8th beta sheet), including the phosphate binding site for ATP (< 235 a.a.)

(Kull et al. 1996; Sablin et al. 1996) was extracted. Sequences of human, yeast and fruit fly kinesin proteins belonging to the "kinesin-14A" subfamily were extracted by the same procedures. A phylogenetic tree was drawn using Clustal W program version 1.83 (http://clustalw.ddbj.nig.ac.jp/). Bootstrap values (%) were obtained for 1,000 pseudoreplicate datasets. Kinesin-5 proteins of human and yeast were used as an outgroup (see Fig. 1A). Coiled-coil regions in Fig. 1B were predicted by SMART (http://smart.embl-heidelberg.de/) and COILS (http://www.ch.embnet.org/software/COILS_form.html).

Gene knockouts

All procedures were performed as described by Dave et al. (2009). *T. thermophila* cell strains, B2086 and CU428 were used for germline transformation. Gene-disrupting plasmids were constructed to target a part of the coding region encoding the C-terminal motor domain of *KIN141* (990 bp, see Fig. 1B) and *KIN142* (see Fig. S1). One hundred μg of a targeting plasmid was digested to remove the plasmid backbone, used to coat gold particles (0.6 μm diameter, BIO-RAD, Hercules, CA) and introduced into cells with PDS-1000/He (BIO-RAD). Genotypes of KO strains were confirmed by diagnostic PCRs that distinguished between the wild-type and disrupted alleles (see Fig. 1C, D). Single KO mutants were crossed to each other and double KO strains were generated with the use of PCR genotyping of outcross progeny Dave et al. (2009).

Tagging with EGFP

All procedures were performed as previously described by Gaertig et al. (1999) and Shang et al. (2002). The taxol-sensitive *T. thermophila* mutant, CU522 strain was used for transgene introduction. The cDNAs of *KIN141* and *KIN142* were expressed as fusions to the *Tetrahymena*-optimized *EGFP* (from Dr. Mochizuki, IMBA, Vienna, Austria) and under the cadmium ion-inducible *MTT1* promoter (see Fig. 2A). To induce transgene expression, 2 μg/ml $CdCl_2$ was added to the culture media. To induce the transgene during conjugation, cadmium-treated growing cells were starved overnight in cadmium-free 10 mM Tris–HCl and mixed.

Indirect immunofluorescence

Cells were fixed as described in Kushida et al. (2011). For double detection of MTs and GFPs, fixed cells were treated with the mouse anti-chicken α-tubulin antibody (Cat# CP06, Calbiochem, Darmstadt, Germany; 1/300 dilution) and the rat anti-GFP antibody (Cat# 04404-26, Nacalai tesque, Kyoto, Japan; 1/300 dilution) at room temperature, overnight. After washing, cells were incubated with the rhodamine-conjugated goat anti-mouse IgG antiserum (Jackson ImmunoResearch Laboratories, West Grove, PA; 1/300 dilution) and the Alexa Fluor 488-conjugated donkey anti-rat IgG antiserum (Life technologies, Junction City, OR; 1/300 dilution) for 6 hr. DNA was stained with DAPI (0.5 μg/ml). Cells were observed under a confocal laser scanning microscope, LSM700 (Carl Zeiss, Oberkochen, Germany) with an alpha Plan-Apochromat 100× lens (N.A. 1.46). For single staining of MTs, fixed cells were treated with the mouse anti-chicken α-tubulin antibody (described above, 1/150 dilution) followed by the incubation with FITC-conjugated goat anti-mouse IgG antiserum (TAGO, Burlingame, CA; 1/150 dilution). DNA was stained with 24 μg/ml propidium iodide for 40 min after the treatment with 0.1 mg/ml RNase for 1 h. Cells were observed under a confocal microscope, LSM510 (Carl Zeiss, Oberkochen, Germany) with an alpha Plan-Fluar 100× lens (N.A. 1.45).

RESULTS

Two mitotic kinesin-14 subfamily genes are present in the *Tetrahymena* genome

An exhaustive phylogenic analysis of kinesins by Wickstead et al. (2010) revealed that *Tetrahymena* has five genes encoding kinesin-14. Two of them (TTHERM_00115410 and TTHERM_00564430, which are named here *KIN141* and *KIN142*, respectively) encode proteins that group with the "kinesin-14A" subgroup that clusters with the *Drosophila* kinesin-14, *Ncd,* the founding member of the kinesin-14 subfamily (Fig. 1A). Microarray studies by Xiong et al. (2013) reveal that relative expression levels of both genes peak at meiosis I during conjugation. The other three *Tetrahymena* kinesin-14 proteins group with the "kinesin-14C" or the "kinesin-14D" subgroups, which intriguingly also includes kinesins that contribute to the function of phragmoplast in plants (Hiwatashi et al. 2008).

EGFP-KIN141 localized at spindle poles during mitosis

EGFP-KIN141-expressing cells grew normally. During vegetative growth, in live cells, there was a diffused signal of EGFP-KIN141 in the cell body and no co-localization with any recognizable structures was seen (data not shown). In an attempt to reduce the background fluorescence, the cells were permeabilized, fixed and processed for immunofluorescence with an anti-GFP antibody. Confocal imaging showed that EGFP-KIN141 co-localized with MTs inside the sphere-shaped interphase MIC (Fig. 2C, $n = 3$). Inside the mitotic micronucleus, EGFP-KIN141 was distributed along the spindle MTs during prophase to metaphase (Fig. 2D, $n = 10$), and concentrated at the spindle poles during anaphase (Fig. 2E, $n = 3$). The signals of EGFP-KIN141 remained on the separation spindle during the late mitotic anaphase (Fig. 2F, $n = 3$). These results suggest that KIN141 migrates toward the spindle poles between the metaphase and anaphase. Despite the presence of a dense network of MTs inside the MAC during amitosis, KIN141 was not detectable inside the MAC (Fig. 2C–E, asterisks, $n = 16$) compared by MIC. Thus, KIN141 preferentially associates with the MTs inside the MIC during mitosis. We could not detect a localization pattern of EGFP-KIN142, besides a diffused signal in the cell body (data not shown).

KIN141 is essential for accurate chromosome segregation during mitosis

Single gene knockout (KO) strains (*KIN141*-KO, *KIN142*-KO) grew at a normal rate (see Fig. S1E). However, a DNA stain showed frequent cases of abnormal chromosome segregation in the mitotic MIC of the *KIN141*-KO cells (Fig. 3D–F, arrowheads). A portion of DNA was often left in the central region of the spindle during the mid and the late anaphase stage (Fig. 3E, asterisk). Consequently, the MIC chromosomes were reconstituted into multiple daughter MICs of unequal sizes. Most of the *KIN141*-KO mutant cells showed defects in the MIC chromosome segregation (86%, $n = 36$, Table 1). While 100% of wild-type cells produced two daughter MICs, in the *KIN141*-KO cells, the number of daughter MICs was two (53%, $n = 36$) or three (39%, $n = 36$), and sometimes more than three (8%, $n = 36$; Fig. 4A). As the consequence of this unequal segregation of MIC chromosomes, the sizes of daughter MICs varied greatly in the *KIN141*-KO cells (Fig. 4B). Compared to the daughter MICs of the wild-type ($4.69 \pm 0.39\ \mu m^2$), the average size of the daughter MICs of *KIN141*-KO was reduced ($3.38 \pm 1.00\ \mu m^2$). Importantly, virtually all daughter cells of *KIN141*-KO cell possessed a detectable MIC chromosome ($n = 39$, see Fig. 4C), which indicates that KIN141 is not essential for mitotic chromosome segregation but is required for its accuracy. During *Tetrahymena* mitosis, the MIC assumes a spindle-like shape from the early stage of prophase (as reviewed in Cole and Sugai 2012). Notably, the mitotic spindle looked normal at the beginning of the mitotic prophase in *KIN141*-KO cells (Fig. 3C, arrow). The length of the mitotic spindle in *KIN141*-KO mutants was about the same as in the wild-type (Fig. 4D). In contrast to the profound mitotic defects, the organization of MTs (Fig. 3D, arrow) and the partition of DNA (Fig. 3F, asterisks) during amitosis of the MAC seemed normal in the *KIN141*-KO cells. A knockout of *KIN142* did not produce a detectable phenotype during the vegetative life cycle and the phenotype of the double KO strain was similar to the phenotype of the *KIN141*-KO strain. To conclude, while *KIN142* is dispensable, *KIN141* has a major contribution to the organization of mitotic spindle and accurate chromosome segregation during mitosis.

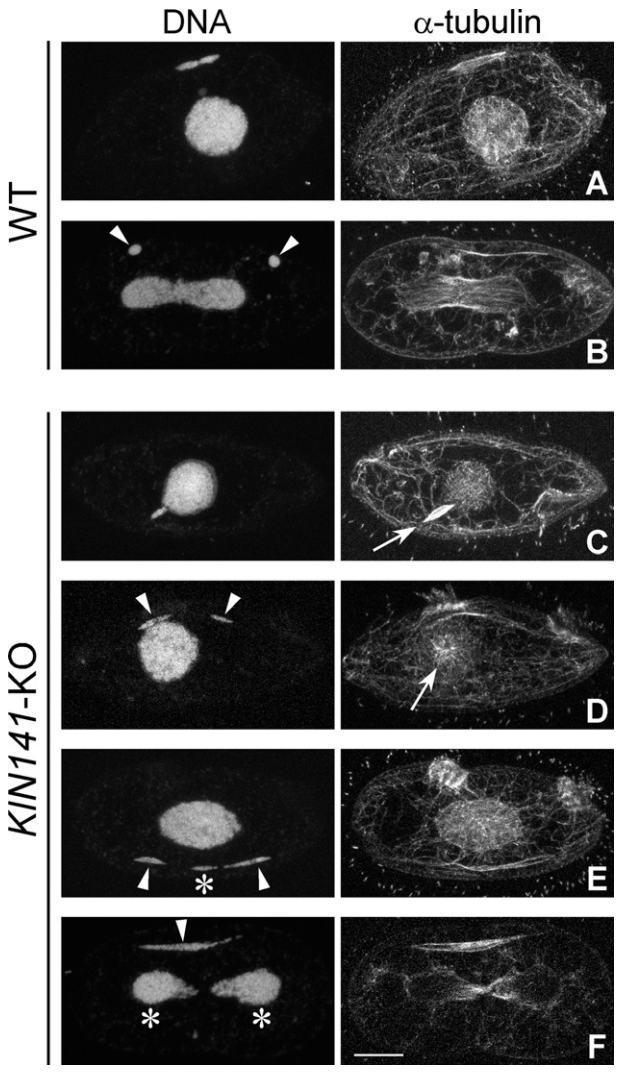

Figure 3 Phenotypes of *KIN141*-KO mutants during vegetative stage of the life cycle. Immunofluorescence images for anti-α-tubulin are shown. DNA is stained with DAPI. (**A**) Early mitotic anaphase of a wild-type cell. (**B**) Late mitotic anaphase of a wild-type cell. MIC DNAs segregate equally to the daughter MICs (arrowheads). (**C**) Mitotic prophase in the *KIN141*-KO mutants. The spindle is marked by an arrow. (**D**) Mitotic anaphase in the *KIN141*-KO mutant. The MIC chromosomes segregate unequally (arrowheads). In the MAC, the amitotic MTs look normal (arrow). (**E**) Mitotic anaphase in the *KIN141*-KO mutant. The MIC chromosomes segregate unequally (arrowheads), and some chromosomes remain in the middle of spindle (asterisk). (**F**) A defective mitosis without chromosome segregation. MIC chromosomes fail to segregated (arrowhead) while the MAC chromosomes segregated normally (asterisks). Scale bar: 10 μm.

EGFP-KIN141 localized at the spindle poles during meiosis

The early stages of *Tetrahymena* conjugation including meiosis have been described extensively by visualizing the MIC DNA (Kaczanowski et al. 1985; Loidl and Mochizuki 2009; Loidl and Scherthan 2004; Martindale et al. 1982;

Table 1. The mitotic phenotypes of *Tetrahymena KIN141* gene KO mutants

Strains	Normal (%)	Abnormal (%)
WT (B2086) ($n = 8$)	100	0
KIN141-KO ($n = 36$)	14	86
KIN142-KO ($n = 35$)	100	0
KIN141&142-KO ($n = 40$)	15	85

Cells were classified into "normal" (see Fig. 3B) or "abnormal" (see Fig. 3D–F) depending on their chromosome segregation patterns. *KIN141*-KO and *KIN141&142*-KO cells had a similar mutant phenotype while the *KIN142*-KO cells were normal.

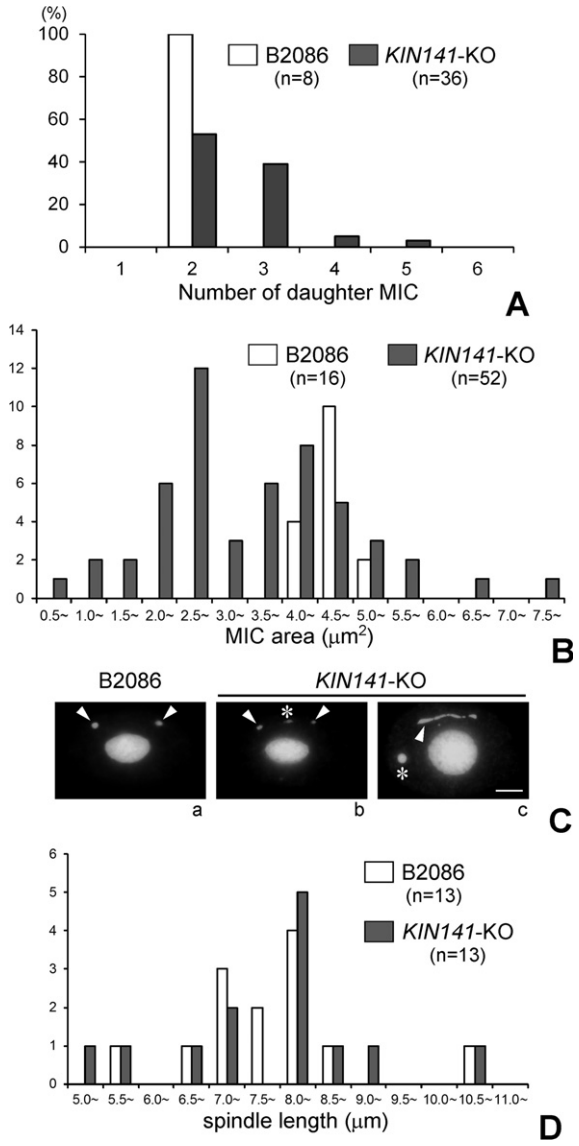

Figure 4 The number and size distribution of the MICs during vegetative growth. (**A**) The number of daughter MICs produced by mitosis. While invariably two daughter MICs are produced by a WT mitosis (white bar), the *KIN141*-KO mutants frequently produce three or more daughter MICs during mitosis (gray bars). (**B**) The size distribution of MICs in WT (white bars) and *KIN141*-KO cells (gray bars). Compared to the WT strain B2086 (4.69 ± 0.39 μm^2), the MICs of the *KIN141*-KO mutants are smaller (3.38 ± 1.00 μm^2) and more varied in size. (**C**) DAPI staining of DNA of WT and *KIN141*-KO cells during mitosis. (a) A WT cells. Arrowheads indicate the daughter MICs of equal size. (b) A *KIN141*-KO cell. Arrowheads indicate the daughter MICs of different sizes. The asterisk indicates a MIC chromosome that failed to segregate and remained in the central region of the spindle between the daughter MICs. (c) A *KIN141*-KO cell. The arrowhead indicates an unsegregated MIC chromosome. The asterisk indicates an abnormal DNA segment in cytoplasm. Scale bar: 10 μm. (**D**) The effect of KIN141 loss on the mitotic spindle length. The distribution of the mitotic spindle lengths of WT (white bars) and *KIN141*-KO cells (gray bars). All measurements were done at the stage corresponding to mitotic prophase to metaphase. There is no statistically significant difference between the two strains ($p > 0.05$).

Mochizuki et al. 2008; Ray 1956; Sugai and Hiwatashi 1974), MIC MTs (Gaertig and Fleury 1992; Wolfe et al. 1976), and MIC nuclear envelope (Cole and Sugai 2012), which are summarized in Fig. 5A, B. To start conjugation, two cells of complementary mating types connect (through the conjugation junction), and enter meiosis I. The changes of the MIC during the meiotic prophase are described as six stages (stages I–VI). The spherical MIC swells and then detaches from the pocket of the MAC (stage I) and starts to elongate to form a long, thread-like MIC called the crescent (stages II–IV). During stage IV, the pairing of the homologous chromosomes takes place. Then, the crescent MIC starts to shorten coincident with chromosome condensation (stages V and VI), and a bipolar meiotic spindle is formed (Metaphase I). At the end of two meiotic divisions (meiosis I and II), four haploid MICs are formed (Anaphase II), and one of them moves to the conjugation junction and becomes selected for following events (namely, the nuclear exchange through conjugation junction, followed by the fertilization and the nuclear differentiation).

We addressed the localization of KIN141 during meiosis using immunofluorescence (Fig. 6A–F) and live imaging (Fig. 6G–I) of early mating cells. An EGFP-KIN141-expressing and a wild-type strain of different mating types were starved and mixed to induce conjugation. The signal of EGFP-KIN141 was already detectable along the MTs in the MICs of both the EGFP-KIN141 partner and the wild-type

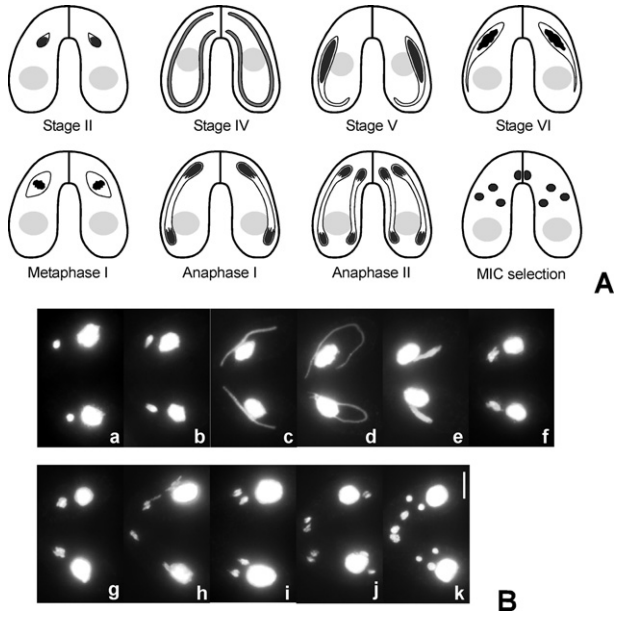

Figure 5 The early stages of *Tetrahymena* conjugation. (**A**) Schematic diagram of the early stages of conjugation as described by Sugai and Hiwatashi (1974), Martindale et al. (1982), and Cole and Sugai (2012). MIC chromosomes are shown in dark gray. The parental MAC is shown in light gray. (**B**) DAPI staining images of the early stages of conjugation Scale bar: 10 μm. (a) stage I, (b) stage II, (c) stage III, (d) stage IV, (e) stage V, (f) stage VI to diakinesis, (g) metaphase I, (h) anaphase I, (i) metaphase II, (j) anaphase II, (k) MIC selection.

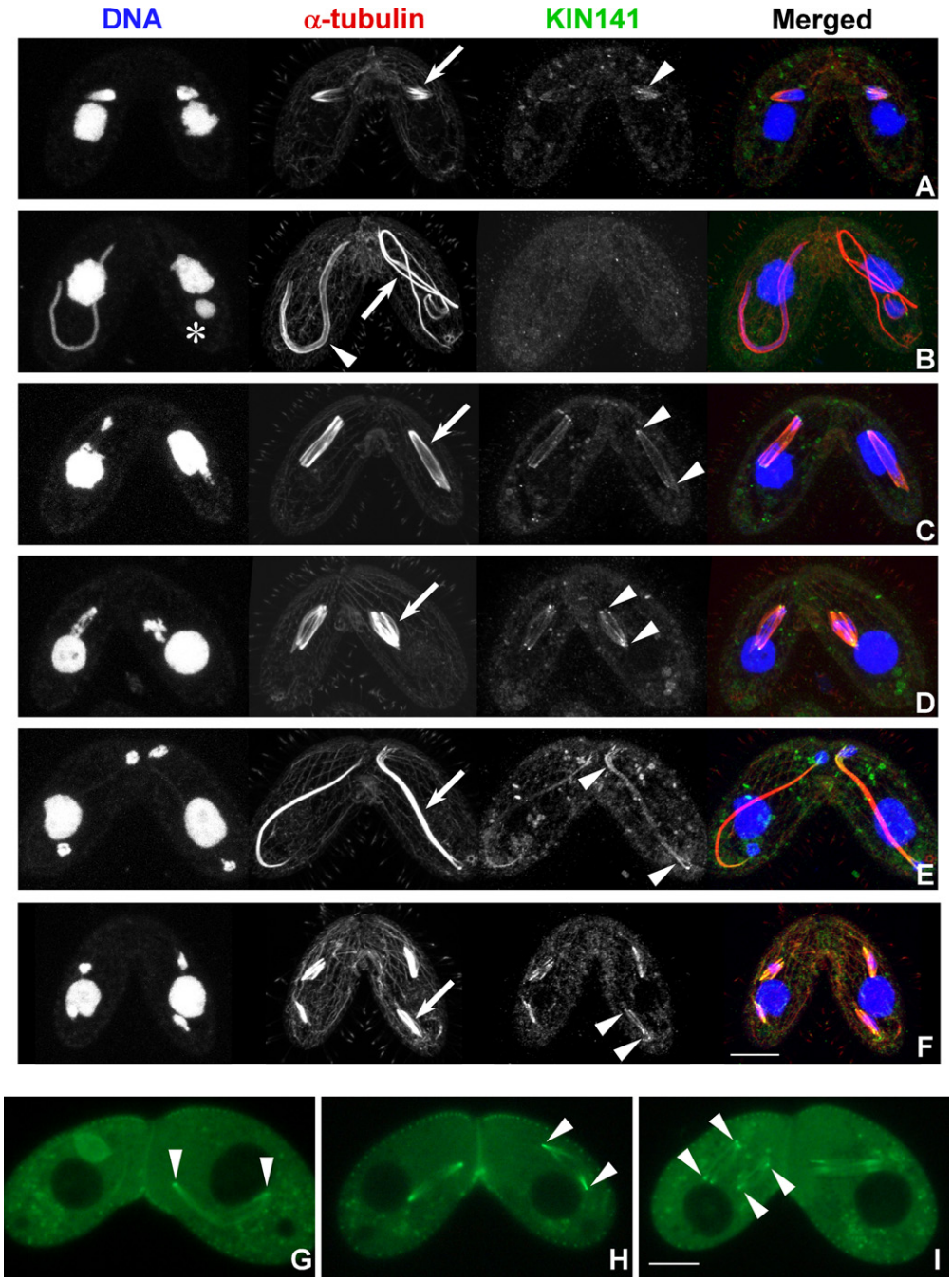

Figure 6 Localization of EGFP-KIN141 during conjugation. Wild-type and EGFP-KIN141-overproducing strains of different mating types were allowed to conjugate (and form EGFP-KIN141 × WT pairs) and analyzed with immunostaining using anti-α-tubulin and anti-GFP antibodies (**A**–**F**) and subjected to live imaging (**G**–**I**). In all panels, arrows indicate the MIC MTs. (A) An early prophase of meiosis I. EGFP-KIN141 localized along the MIC MTs (arrowhead). (B) Middle prophase of meiosis I. Crescent MTs are present (arrowhead) and the MIC has elongated more than the body length resulting in its curvature (crescent stage). In one of the mating partners, the MIC chromosomes failed to elongate (asterisk) but the MIC MTs have elongated (arrow) in the same nucleus during the crescent stage. (C) A late prophase of meiosis I. EGFP-KIN141 accumulated at the both ends of the shortening crescent (arrowheads). (D) Metaphase of meiosis I. EGFP-KIN141 accumulates at the spindle poles (arrowheads). (E) Anaphase of meiosis I. KIN141 remains near the spindle poles (arrowheads). (F) Metaphase of meiosis II. EGFP-KIN141 accumulates at both spindle poles (arrowheads). Scale bars: 10 μm. (G) Prophase of meiosis I. EGFP-KIN141 localizes to both ends of the shortening crescent MIC (arrowheads). The crescent fails to elongate in one partner of the pair (likely the cell carrying the EGFP-KIN141-overexpressing transgene) (left cell). (H) Metaphase of meiosis I. EGFP-KIN141 accumulates at the spindle poles (arrowheads). (I) Metaphase of meiosis II. EGFP-KIN141 accumulated at spindle poles (arrowheads). Scale bars: 10 μm.

partner at the onset of meiosis I (Fig. 6A, $n = 10$), indicating that EGFP-KIN141 diffuses rapidly between the mating partners. At the prophase of meiosis I, the MIC chromosomes are relatively decondensed and homologous chromosomes undergo pairing (Kaczanowski et al. 1985; Loidl and Scherthan 2004). During this period, the entire MIC elongates to reach the length of about twice the cell body length ("crescent" stage). Soon after the completion of chromosome paring, the crescent MIC shortens to about one-third of the cell body length and the meiotic spindle is formed (Loidl and Scherthan 2004). Frequently, during the crescent stage, MTs were abnormally organized (Fig. 6B, arrow) and the elongation of crescent DNA failed (Fig. 6B, asterisk, 74%, $n = 19$) only on one side of the mating pair, presumably the side that expressed EGFP-KIN141. Next, EGFP-KIN141 accumulated at the both ends of the shortening crescent MTs. This pattern of localization was confirmed by both immunofluorescence (Fig. 6C, $n = 9$) and live cell imaging (Fig. 6G, $n = 3$). EGFP-KIN141 also accumulated at the spindle poles at the metaphase (diakinesis) of meiosis I (Fig. 6D, H, $n = 11$ and 6, respectively). The EGFP-KIN141 signal remained on MTs near the spindle poles during the anaphase of meiosis I (Fig. 6E, $n = 2$), and reappeared at the spindle poles during the metaphase of meiosis II (Fig. 6F, I, $n = 2$ and 5, respectively).

KIN141 is essential for MIC chromosome segregation during meiosis I

The phenotype of mating *KIN141*-KO × *KIN141*-KO cells during meiosis (Fig. 7A′–H′) was analyzed by immunofluorescence and compared with a wild-type (WT) × WT cross (Fig. 7A–H). The conjugation stage timing of the *KIN141*-KO × *KIN141*-KO cross-seemed normal (see Fig. S2). During early prophase of meiosis I, the crescent MICs of *KIN141*-KO × *KIN141*-KO pairs elongated normally (Fig. 7A′, B′, arrows). However, the shortening of the crescent MTs was delayed in the *KIN141*-KO × *KIN141*-KO pairs (Fig. 7C′, arrow). The ends of shortening crescent MTs were excessively sharp (Fig. 7C′, arrow) compared with the ends of the wild-type crescent MTs (Fig. 7C, arrow, see Table 2). At the metaphase of meiosis I, the spindle had unfocused MTs extending from one or both spindle poles (Fig. 7D′, arrows). While at the metaphase I stage, the spindle length was normal in the WT × WT cross and the WT × *KIN141*-KO crosses, the *KIN141*-KO × *KIN141*-KO cells had excessively long spindles (Fig. 8A, B). The spindles remained long also during anaphase I (Fig. 7E, E′, arrows). The condensed MIC chromosomes in the disorganized meiotic spindle of *KIN141*-KO × *KIN141*-KO pairs were dispersed, and eventually, the knockout pairs displayed an irregular (seemingly random) chromosome partition during meiosis (Fig. 7E′, arrowheads). The movement of chromosomes between MT bundles in *KIN141*-KO × *KIN141*-KO pairs seemed highly erratic because sometimes all chromosomes were left at one end of the MT bundle and not partitioned at all (Fig. 7E′, left cell). Unlike an effective segregation of MIC chromosomes during meiosis I of WT × WT pairs (Fig. 9A), chromosomes were left in the middle of the meiotic spindle of *KIN141*-KO × *KIN141*-KO pairs (Fig. 9B), which produced multiple daughter MICs (Fig. 9C). Meiosis II seemed to either fail or be abnormal in the *KIN141*-KO × *KIN141*-KO pairs. At the end of meiosis I, nuclear MTs were visible but they were not organized into a proper spindle (Fig. 7F′, arrow). The anaphase of meiosis II was recognizable by the formation of multiple long MT bundles but 90% of the MICs ($n = 21$) failed to segregate chromosomes equally (Fig. 7G′). The selection of a single postmeiotic MIC following meiosis was often observed, but neither the size nor the number of meiotic products seemed normal (Fig. 7F′–H′, arrowheads). This phenotype demonstrated that *KIN141* is essential for the formation of proper meiotic spindle and meiotic chromosome segregation. Notably, the meiotic spindle is much longer (22.5 ± 5.7 μm, see Fig. 8A) as compared to the mitotic spindle (7.9 ± 1.4 μm, see Fig. 4D) in the *KIN141*-KO cells.

DISCUSSION

Clearly, the *KIN141* kinesin-14 plays an important role in chromosome segregation during both mitosis and meiosis, but not during amitosis, a process that also involves intranuclear MTs which are not organized into a bipolar spindle.

In other organisms, kinesin-14 is a dimeric, nonprocessive, minus-end-directed MT motor (Chandra et al. 1993; McDonald et al. 1990; Pechatnikova and Taylor 1997, 1999; Tao et al. 2006). KIN141 has a C-terminally located motor domain (Fig. 1B), a conserved feature associated with a minus-end directionality (Chandra et al. 1993; McDonald et al. 1990; Pechatnikova and Taylor 1997, 1999). Thus, KIN141 is likely also a minus-end directed motor. Thus, KIN141 could accumulate at the minus-ends of MTs (i.e. near the poles of both the mitotic (Fig. 2E) and meiotic spindle (Fig. 6D)) via its minus-end-directed motor activity.

The *KIN141*-KO mutants display severe defects in the organization and function of the meiotic spindle. The MT-driven elongation of the prophase I MIC to twice the length of the cell (crescent stage) is a characteristic feature of oligohymenophorean ciliates such as *Paramecium* (Stevenson 1972) and *Tetrahymena* (Ray 1956). The meiotic crescent stage is believed to be important for the successful pairing of homologous chromosomes (Kaczanowski et al. 1985; Loidl and Scherthan 2004). Following the crescent stage, the chromosome condensation and the MIC shortening occur quickly to form a meiotic spindle (Gaertig and Fleury 1992; Kushida et al. 2015). Our study shows that the shortening of the MIC crescent MTs is defective in the absence of *KIN141* (Fig. 7D′) and consequently the length of the meiotic spindle is increased twofold as compared to the wild-type at the same stage (Fig. 8). It appears that the crescent shortening involves two activities, namely, a KIN141-dependent shortening, likely driven by its motor activity and a KIN141-independent shortening that could involve MT depolymerization.

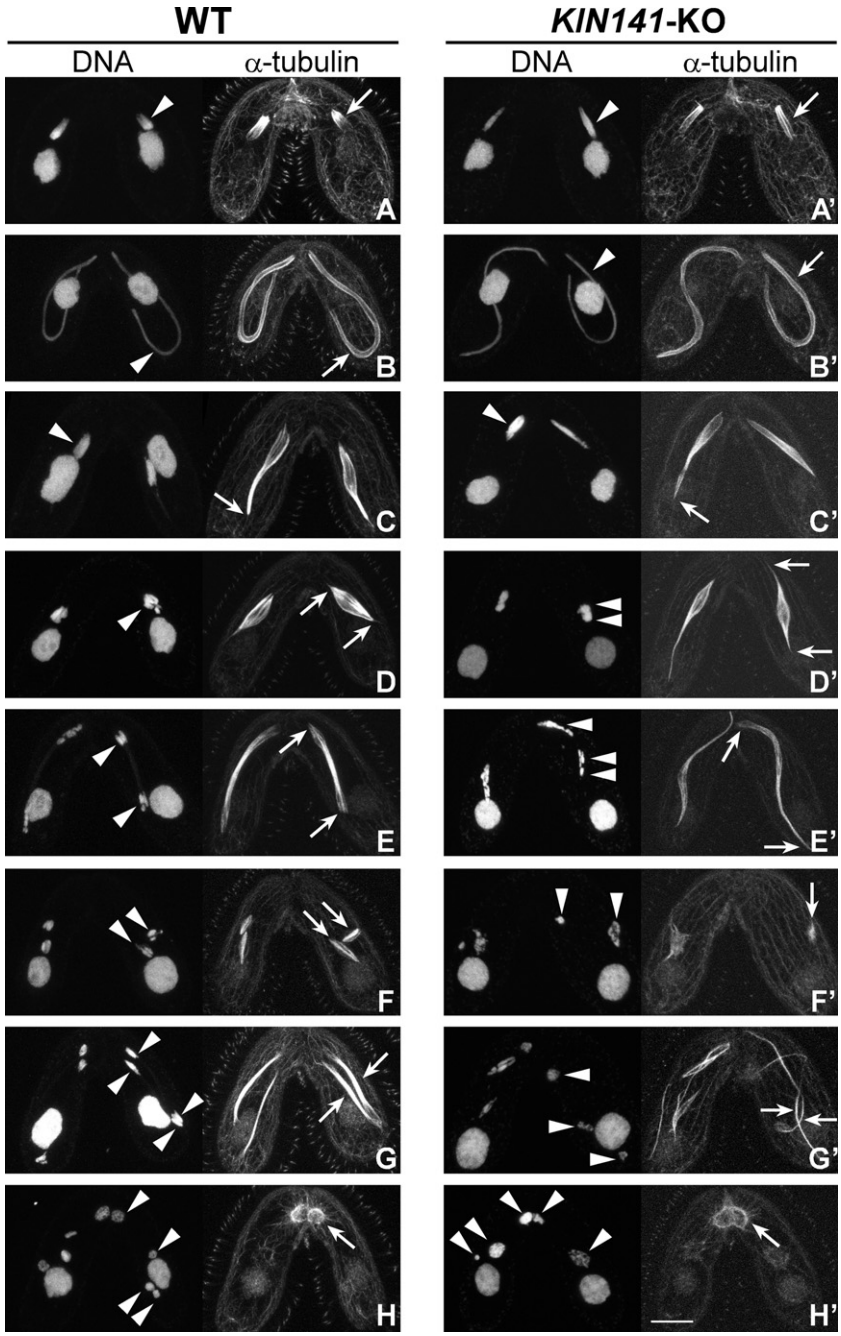

Figure 7 The MIC phenotypes during *KIN141*-KO × *KIN141*-KO conjugation. Immunofluorescence images for anti-α-tubulin are shown. DNA is stained with DAPI. *KIN141*-KO × *KIN141*-KO phenotypes (**A′–H′**) were compared with a WT × WT conjugation (**A–H**). In all panels, arrows and arrowheads indicate the MIC MTs and the MIC chromosomes, respectively. (A) An early prophase of meiosis I. The crescent MIC starts to elongate. (B) A middle prophase of meiosis I. The crescent MIC reached the full length. (C) A late prophase of meiosis I. The shortening end of the crescent is round-shaped (arrow). (D) A metaphase of meiosis I. Both spindle poles are tightly focused and almost all MTs are collected in between spindle length (arrows). (E) An anaphase of meiosis I. The MIC chromosomes have segregated equally (arrowheads). (F) A metaphase of meiosis II. (G) An anaphase of meiosis II. (H) A postmeiotic nuclear selection. Four postmeiotic MICs are present (arrowheads). The arrow indicates the MTs near the single selected MIC. (A′) An early prophase of meiosis I. (B′) A middle prophase of meiosis I. The crescent MIC has elongated normally in the *KIN141*-KO × *KIN141*-KO pairs (arrow and arrowhead). (C′) A late prophase of meiosis I. The shortening end of the crescent is excessively sharp (arrow) (D′) An apparent metaphase of meiosis I. Note MTs that fail to focus properly (arrows). The spindle is abnormally long (see Fig. 9A). Two clumps of chromosomes were usually observed in the *KIN141*-KO MICs (arrowheads). (E′) A likely anaphase of meiosis I. The mitotic spindle is excessively long (arrows) and the MIC chromosomes have failed to segregate equally (arrowheads). (F′) The nuclei that are products of meiosis I. Sometimes, the MTs can be detectable in the MIC (arrow), which resembles an aster more than a spindle. (G′) The stage corresponding to the anaphase of meiosis II. The multiple MT bundles (arrows), which seem nonfunctional for chromosome segregation (arrowheads), are formed. (H′) A postmeiotic nuclear selection stage. Arrowheads indicate postmeiotic MICs. Scale bar: 10 μm.

Strikingly, the meiotic spindles of the *KIN141*-KO mutants have excessively sharp ends (Fig. 7D', arrows) compared to the relatively blunt ends of the wild-type spindle (Fig. 7D arrows). These results suggest that *KIN141* gathers the ends of MIC MTs at MIC ends during the crescent shortening. In other organisms, the mitotic kinesin-14 is known to gather the minus-ends of spindle MTs near the spindle poles (Cross and McAinsh 2014). This phenomenon, called the "minus-end focusing", produces a diamond-shaped spindle (Goshima et al. 2005). The minus-end focusing is a result of both MT cross-linking and MT sliding activity of the minus-end-directed motor domain of kinesin-14 (Burbank et al. 2007; Cai et al. 2009; Fink et al. 2009; Goshima et al. 2005; Hepperla et al. 2014; Sharp et al. 1999). Thus, KIN141 may drive MT sliding during the shortening of the crescent. In the *KIN141*-KO mutant cells, the poles of meiotic spindle-like MT structure fail to focus completely, and tail-like MT bundles extend from both or one end of spindle. These abnormally long meiotic spindles also are associated with defects in chromosome segregation during anaphase I. Thus, our observations show that *KIN141* contributes to meiotic processes of crescent shortening, bipolar spindle formation and chromosome segregation. It is worth mentioning that the intranuclear spindles of ciliates including *Tetrahymena* lack centrosomes (Davidson and LaFountain 1975; LaFountain and Davidson 1979, 1980) as in higher plants (Clayton et al. 1985; Schmit et al. 1983; Wasteneys 2002) or in the meiotic spindle of vertebrates (Albertson and Thomson 1993; Clift and Schuh 2013; Gard 1992; Schuh and Ellenberg 2007; Theurkauf and Hawley 1992). Notably, the difference between meiotic and mitotic spindle length was increased more than twofold in the *KIN141*-KO cells, compared to wild-type cells (13.9 ± 1.7 μm vs. 7.9 ± 1.2 μm). If the random segregation of the chromosome takes place in the KIN141-KO cells, the longer spindle possibly increases the chance of irregular segregation of MIC to several unequal sizes because chromosomes are need to travel longer way during segregation. Such a difference in spindle length may be the reason that the chromosome segregation during meiosis was more severely disturbed (100%, $n = 20$, see Fig. 9B) than during mitosis (86%, $n = 36$, see Table 1). Moreover, the inhibition of crescent elongation during meiotic prophase by the overexpression of EGFP-KIN141 (Fig. 6B) suggests that overproduced KIN141 excessively cross-links the nuclear envelope-

Table 2. The defect on meiotic spindle formation of *Tetrahymena KIN141* gene KO mutants

Crosses	Blunt (%)	Sharp (%)
WT × WT ($n = 18$)	72	28
KO × KO ($n = 17$)	6	94

The ends of immunostained shortening crescent MTs were classified into "blunt" (see Fig. 7C, arrow) or "sharp" (see Fig. 7C', arrow) by their shape. In *KIN141* mutants, the most of the ends of shortening crescent MTs were excessively sharp compared with wild-type crescent MTs.

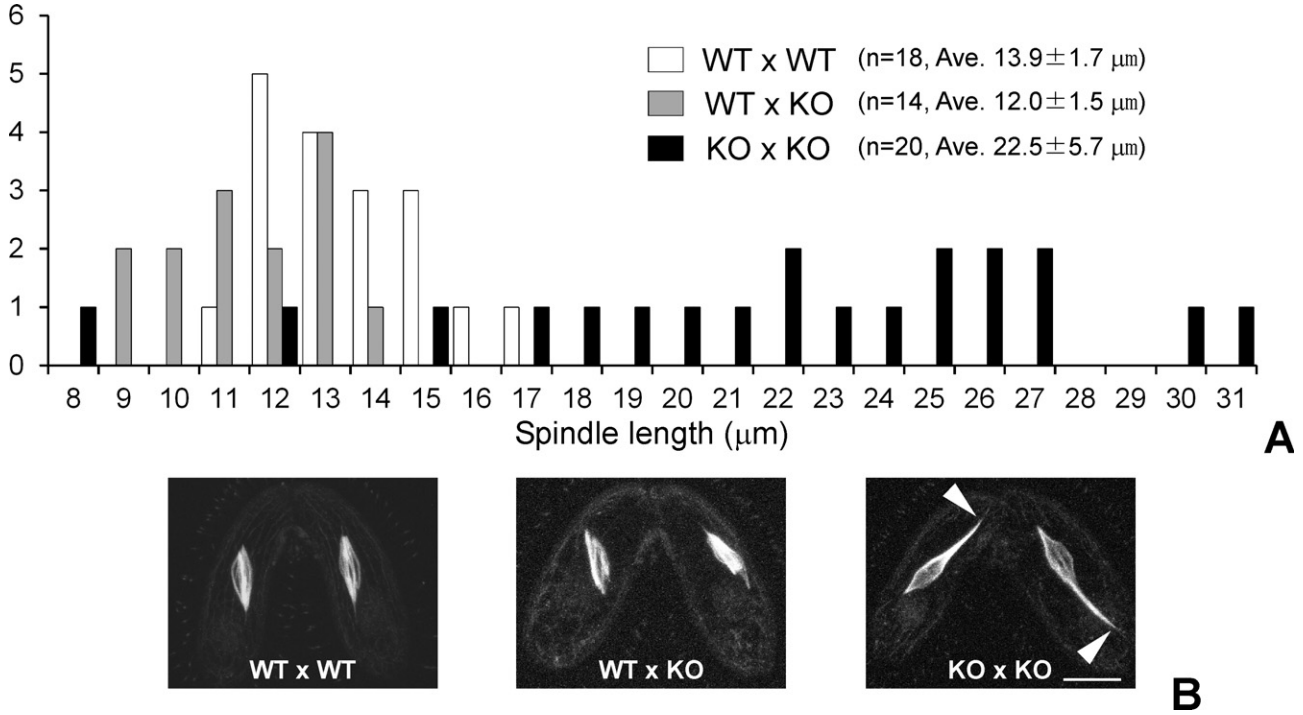

Figure 8 The distribution of spindle lengths during meiosis I. (**A**) In a WT × WT cross (white bars), WT × KO cross (gray bars) and KO × KO cross (black bars). The *KIN141*-KO × *KIN141*-KO pairs have longer meiotic spindles as compared with the pairs containing a WT partner. (**B**) A MT staining of a meiotic spindle of a WT × WT cross, a WT × *KIN141*-KO cross and a *KIN141*-KO × *KIN141*-KO cross. The *KIN141*-KO × *KIN141*-KO pair has longer meiotic spindles with abnormal tails of MTs (arrowheads). Scale bar: 10 μm.

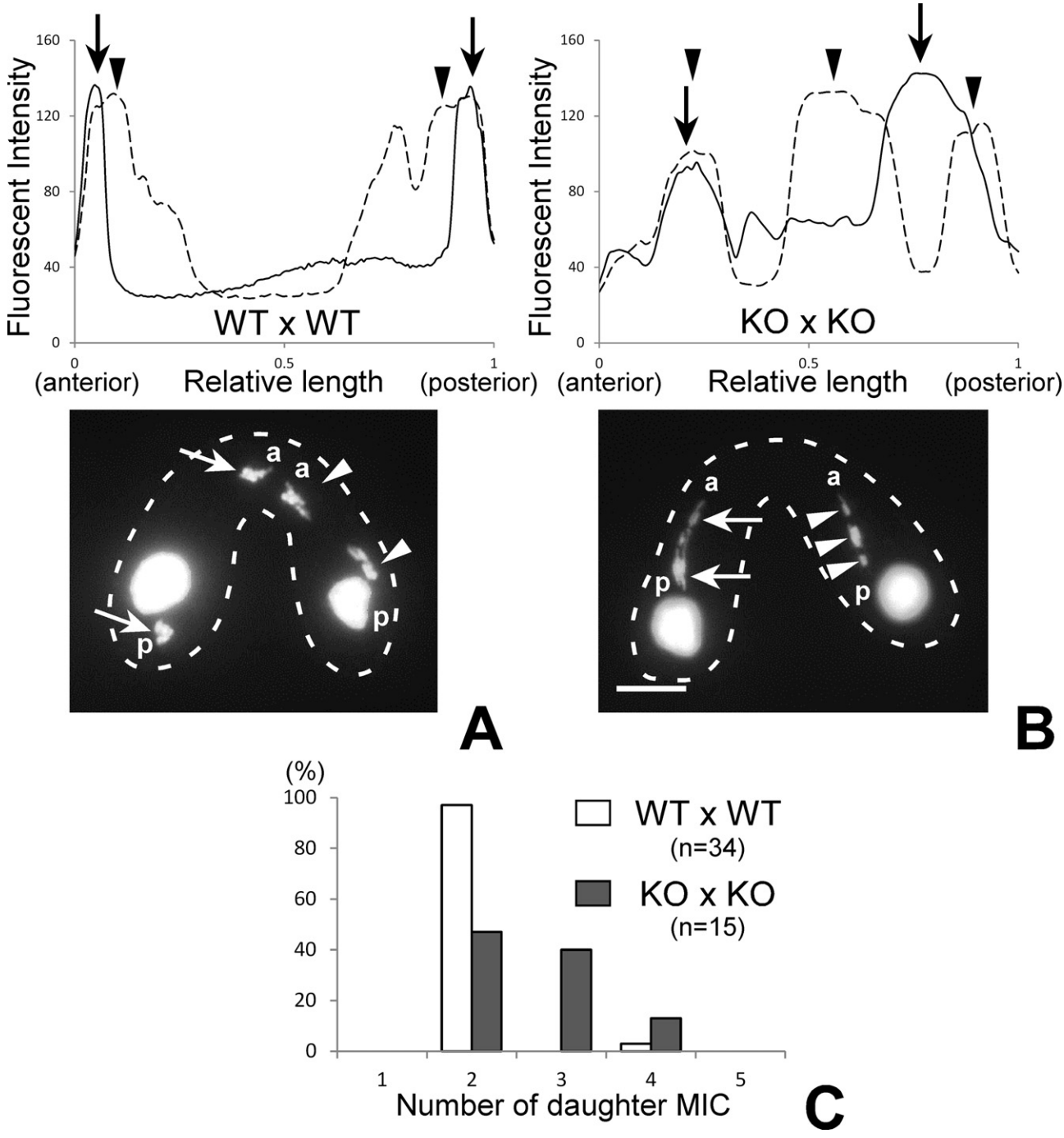

Figure 9 Chromosome segregation defects during meiosis in the *KIN141*-KO mutants. (**A,B**) (Top panels) Line profiles of fluorescent intensity (F.I.) of the MIC chromosomes during anaphase of meiosis I in a WT × WT and a *KIN141*-KO × *KIN141*-KO cross. (Bottom panels) The DAPI images used to generate the profiles F.I. shown above. Solid lines and dashed lines in profiles indicate F.I. in left cell and right cell of the pairs, respectively. While two clear peaks of F.I. are detected at the ends of WT × WT spindles (arrows and arrowheads in panel A), two peaks of unequal height (arrows in panel B) or three peaks (arrowheads in panel B) are present in the middle of the *KIN141*-KO × *KIN141*-KO spindle. In the DAPI images, the outlines of pairs are marked with broken lines, and anterior and posterior ends of the spindles are marked as "a" and "p", respectively. Bar indicates 10 μm. (**C**) Frequency distribution of the number of the daughter MICs during anaphase of meiosis I in WT cross and KO cross.

associated MTs in the crescent stage MIC. Also, the potential malfunction of KIN141 caused by GFP-tagging itself may affect the regulation of crescent elongation.

Our models of contributions of *KIN141* to mitosis and meiosis are summarized in Fig. 10, 11, respectively. Compared to the meiotic bipolar spindle formation, the mitotic

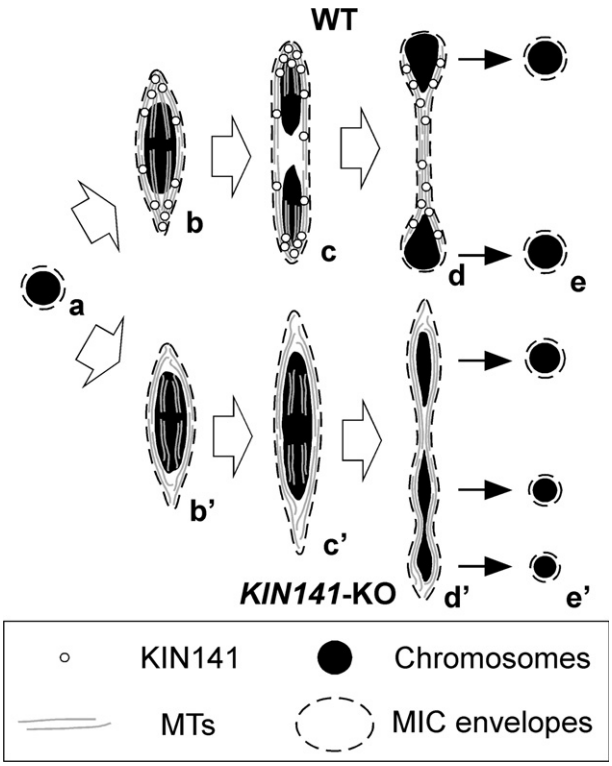

Figure 10 A model for the involvement of KIN141 during mitosis. The distribution of MIC envelopes is adapted from the observations of Cole and Sugai (2012). (**a**) An interphase MIC. (**b**) A mitotic spindle of a WT cell. Both k-fibers and peripheral sheath MTs (psMTs) are cross-linked by KIN141 near the spindle poles. Note that the MIC chromosomes are not located at the equator of the nucleus (Cervantes et al. 2006). (**c**) An early mitotic anaphase of a WT cell. The MIC chromosomes are segregated equally to both daughter MICs pulled by k-fibers. (**d**) A late mitotic anaphase in a WT cell. KIN141 remains on the MT bundles of the dumbbell-shaped MIC. (**e**) The daughter MICs after a WT mitosis. All MIC chromosomes are segregated to either daughter MICs of equal size. (**b'**) A defective mitotic spindle in a *KIN141*-KO cell. The k-fibers and interpolar MTs are uncoupled. (**c'**) An early mitotic anaphase in a *KIN141*-KO cell. The k-fibers cannot pull chromosomes sufficiently apart because they are not attached to the spindle poles. (**d'**) A late mitotic anaphase of *KIN141*-KO cell. The MIC envelope-associated MTs start to bundle together to form a "separation spindle", and the MIC chromosomes are randomly separated into multiple small MICs. (**e'**) The daughter MICs of mitosis of *KIN141*-KO cell. The size and number of daughter MICs are varied.

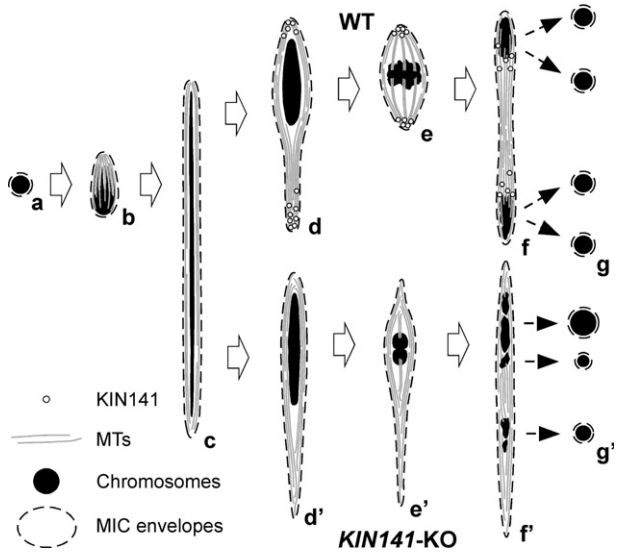

Figure 11 A model of involvement of KIN141 during meiosis I. The distribution of MIC envelopes is adapted from the observations of Cole and Sugai (2012). (**a**) A sphere MIC prior to meiosis. (**b**) A beginning of the crescent elongation during the meiotic prophase. (**c**) A completion of the crescent elongation. The MIC envelope-associated MT bundles form the long string-like crescent MIC. (**d**) Spindle pole formation during the shortening of the crescent MIC in WT cells. KIN141 cross-links the MTs and drives MT sliding that leads to rapid shortening of the crescent. The MIC has thick and round-shaped ends as a result of effective bundling of the MT ends at both spindle poles. (**e**) A meiotic metaphase in a WT cell. KIN141 cross-links spindle MTs near both poles, and fixes the minus-ends of k-fiber bundles to both spindle poles. (**f**) A meiotic anaphase I in a WT cell. The MIC chromosomes are segregated equally to both daughter MICs. (**g**) The outcome of both meiotic divisions in a WT pair. Four postmeiotic MICs of equal size are produced (indicated by arrows) following meiosis I. (**d'**) The shortening of the crescent MIC in *KIN141*-KO cells. The MIC has sharp ends due to lack of pole gathering activity of KIN141. (**e'**) A metaphase I in a *KIN141*-KO cell. The meiotic spindle has long tail-like MT bundles left behind due to lack of MT cross-linking activity of KIN141. The ends of k-fibers are not fixed to the spindle poles. (**f'**) An anaphase I in a *KIN141*-KO cell. The K-fibers fail to segregate chromosomes equally because of the lack of proper attachment to the spindle poles. (**g'**) The outcome of both meiotic divisions in a *KIN141*-KO pair. A disrupted meiosis I eventually leads to multiple MICs of varied sizes.

spindle becomes a spindle-like shape from the very early stage of mitotic prophase in a *KIN141*-independent manner (see Fig. 3C, arrow). This result leads us to conclude that the possible function of KIN141 is to connect the kinetochore MTs (k-fibers) to the network of minus-end-focused spindle MTs including psMTs during mitosis (Fig. 10b, c). In the *KIN141*-KO cell, the ends of k-fibers are not connected to the MT-network (Fig. 10b', c'), and the MIC chromosomes are passively grouped into multiple MICs of unequal sizes (Fig. 10d', e') by bundling of the MIC MTs. This model explains the disrupted chromosome distribution during mitosis of *KIN141*-KO cells. During meiosis, KIN141 may gather the ends of MTs during the crescent shortening (Fig. 11d, 12A, large arrow), and similarly both focus the spindle poles and fix the k-fibers (Fig. 11e, 12A) to ensure equal chromosome segregation (Fig. 11f). Conversely, the disruption in the minus-end focusing in *KIN141*-KO cells result in the longer spindle with sharp ends (Fig. 11e', 12B). The crescent elongation (Fig. 11c) may aggravate the bipolar spindle formation defect in the *KIN141*-KO cells (Fig. 11d'), so that the spindle has long unfocused MTs extended from spindle poles (Fig. 11e'). Such abnormally shaped spindles totally lose the function to segregate chromosomes (Fig. 11f', g').

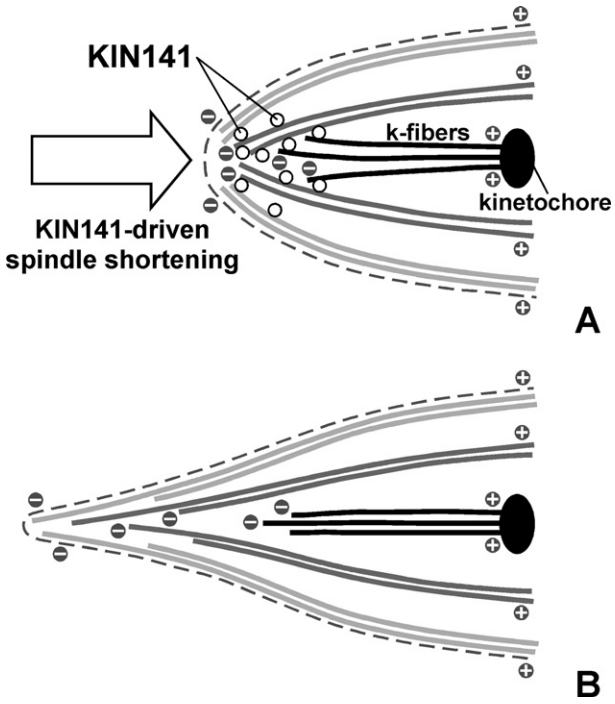

Figure 12 A model of the contribution of KIN141 on the shortening of meiotic crescent. The spindles during metaphase of meiosis I are shown. Solid lines represent the bundles of overlapping MTs. The distribution of MIC envelopes (dashed lines) is adapted from the observations of Cole and Sugai (2012). The polarity of MTs are indicated by "plus (+)" and "minus (−)". (**A**) In WT × WT pair, KIN141 anchored the minus-ends of k-fibers to the network of spindle MTs near the pole (corresponding to Fig. 11, e). A "minus-end focusing" caused by KIN141 during the shortening of crescent eventually shortens the spindle length as indicated by large arrow. (**B**) In *KIN141*-KO × *KIN141*-KO pair, the minus-ends of groups of MTs are not "focused" during and after the crescent shortening (corresponding to Fig. 11e'). Scattered minus-ends of MTs form the long tail-like configuration with the sharp end at the pole of the meiotic spindle.

To summarize, our results show that in *Tetrahymena* KIN141 kinesin-14 localizes to the spindle MTs, in particular at the spindle poles, and is essential for accurate chromosome segregation during both mitosis and meiosis. Especially during meiosis, the stage when the expression of KIN141 is upregulated, KIN141 contributes to the shortening of the prophase crescent stage MIC.

ACKNOWLEDGMENTS

We thank Dr. Kazufumi Mochizuki (IMBA, Vienna, Austria) for donating the *EGFP*-overexpressing and neo4 plasmids. This study was supported by the NIH (RO1GM089912) grant to J.G. and the Sumitomo Foundation and the Novartis Foundation to K.N. This work was supported by the funding from "Promotion program on international collaborative education and research for students and young scientists" of Graduate School of Life and Environmental Sciences, University of Tsukuba to Y.K., which is adopted by Institutional Program for Young Researcher Overseas Visits of Japan Society for the Promotion of Science (JSPS).

LITERATURE CITED

Akematsu, T., Pearlman, R. E. & Endoh, H. 2010. Gigantic macroautophagy in programmed nuclear death of *Tetrahymena thermophila*. *Autophagy*, 6:901–911.

Albertson, D. G. & Thomson, J. N. 1993. Segregation of holocentric chromosomes at meiosis in the nematode, *Caenorhabditis elegans*. *Chromosome Res.*, 1:15–26.

Allen, S. & Gibson, I. 1972. Genome amplification and gene expression in the ciliate macronucleus. *Biochem. Genet.*, 6:293–313.

Burbank, K. S., Mitchison, T. J. & Fisher, D. S. 2007. Slide-and-cluster models for spindle assembly. *Curr. Biol.*, 17:1373–1383.

Cai, S., Weaver, L. N., Ems-McClung, S. C. & Walczak, C. E. 2009. Kinesin-14 family proteins HSET/XCTK2 control spindle length by cross-linking and sliding microtubules. *Mol. Biol. Cell*, 20:1348–1359.

Cervantes, M. D., Xi, X., Vermaak, D., Yao, M. C. & Malik, H. S. 2006. The CNA1 histone of the ciliate *Tetrahymena thermophila* is essential for chromosome segregation in the germline micronucleus. *Mol. Biol. Cell*, 17:485–497.

Chandra, R., Salmon, E. D., Erickson, H. P., Lockhart, A. & Endow, S. A. 1993. Structural and functional domains of the Drosophila ncd microtubule motor protein. *J. Biol. Chem.*, 268:9005–9013.

Clayton, L., Black, C. M. & Lloyd, C. W. 1985. Microtubule nucleating sites in higher plant cells identified by an auto-antibody against pericentriolar material. *J. Cell Biol.*, 101:319–324.

Clift, D. & Schuh, M. 2013. Restarting life: fertilization and the transition from meiosis to mitosis. *Nat. Rev. Mol. Cell Biol.*, 14:549–562.

Cole, E. & Sugai, T. 2012. Developmental progression of *Tetrahymena* through the cell cycle and conjugation. *In:* Collins, K. (ed.), Methods in Cell Biology, Volume 109, *Tetrahymena thermophila*. Academic Press, San Diego, CA. p. 177–236.

Cross, R. A. & McAinsh, A. 2014. Prime movers: the mechanochemistry of mitotic kinesins. *Nat. Rev. Mol. Cell Biol.*, 15:257–271.

Dave, D., Wloga, D. & Gaertig, J. 2009. Manipulating ciliary protein-encoding genes in *Tetrahymena thermophila*. *In:* King, S. M. & Pazour, G. J. (eds.), Methods in Cell Biology, Volume 93, Cilia: Model Organisms & Intraflagellar Transport. Academic Press, San Diego, CA. p. 1–20.

Davidson, L. & LaFountain Jr, J. R. 1975. Mitosis and early meiosis in *Tetrahymena pyriformis* and the evolution of mitosis in the phylum ciliophora. *Biosystems*, 7:326–336.

Endo, M. & Sugai, T. 2011. Amitotic division of the macronucleus in *Tetrahymena thermophila*: DNA distribution by genomic unit. *Zool. Sci.*, 28:482–490.

Endow, S. A., Henikoff, S. & Soler-Niedziela, L. 1990. Mediation of meiotic and early mitotic chromosome segregation in *Drosophila* by a protein related to kinesin. *Nature*, 345:81–83.

Fink, G., Hajdo, L., Skowronek, K. J., Reuther, C., Kasprzak, A. A. & Diez, S. 2009. The mitotic kinesin-14 Ncd drives directional microtubule-microtubule sliding. *Nat. Cell Biol.*, 11:717–723.

Fujiu, K. & Numata, O. 2000. Reorganization of microtubules in the amitotically dividing macronucleus of *Tetrahymena*. *Cell Motil. Cytoskeleton*, 46:17–27.

Gaertig, J. & Fleury, A. 1992. Spatio-temporal reorganization of intracytoplasmic microtubules is associated with nuclear

selection and differentiation during the developmental process in the ciliate *Tetrahymena thermophila*. *Protoplasma*, 197:74–87.

Gaertig, J., Gao, Y., Tishgarten, T., Clark, T. G. & Dickerson, H. W. 1999. Surface display of a parasite antigen in the ciliate *Tetrahymena thermophila*. *Nat. Biotechnol.*, 17:462–465.

Gard, D. L. 1992. Microtubule organization during maturation of *Xenopus* oocytes: assembly and rotation of the meiotic spindles. *Dev. Biol.*, 151:516–530.

Goshima, G., Nédélec, F. & Vale, R. D. 2005. Mechanisms for focusing mitotic spindle poles by minus end-directed motor proteins. *J. Cell Biol.*, 171:229–240.

Hatsumi, M. & Endow, S. A. 1992. The Drosophila ncd microtubule motor protein is spindle-associated in meiotic and mitotic cells. *J. Cell Sci.*, 103:1013–1020.

Hepperla, A. J., Willey, P. T., Coombes, C. E., Schuster, B. M., Gerami-Nejad, M., McClellan, M., Mukherjee, S., Fox, J., Winey, M., Odde, D. J., O'Toole, E. & Gardner, M. K. 2014. Minus-end-directed Kinesin-14 motors align antiparallel microtubules to control metaphase spindle length. *Dev. Cell*, 31:61–72.

Hiwatashi, Y., Obara, M., Sato, Y., Fujita, T., Murata, T. & Hasebe, M. 2008. Kinesins are indispensable for interdigitation of phragmoplast microtubules in the moss *Physcomitrella patens*. *Plant Cell*, 20:3094–3106.

Ito, J., Lee, Y. C. & Scherbaum, O. H. 1968. Intranuclear microtubules in *Tetrahymena pyriformis* GL. *Exp. Cell Res.*, 53:85–93.

Jaeckel-Williams, R. 1978. Nuclear divisions with reduced numbers of microtubules in *Tetrahymena*. *J. Cell Sci.*, 34:303–319.

Kaczanowski, A., Gaertig, J. & Kubiak, J. 1985. Effect of the anti-tubulin drug nocodazole on meiosis and post-meiotic development in *Tetrahymena thermophila*. *Exp. Cell Res.*, 158:244–256.

Karabay, A. & Walker, R. A. 1999. Identification of microtubule binding sites in the Ncd tail domain. *Biochemistry*, 38:1838–1849.

Karabay, A. & Walker, R. A. 2003. Identification of Ncd tail domain-binding sites on the tubulin dimer. *Biochem. Biophys. Res. Commun.*, 305:523–528.

Karrer, K. 2012. Nuclear dualism. *In:* Collins, K. (ed.), Methods in Cell Biology, Volume 109, *Tetrahymena thermophila*. Academic Press, San Diego, CA. p. 29–52.

Kim, N. & Song, K. 2013. KIFC1 is essential for bipolar spindle formation and genomic stability in the primary human fibroblast IMR-90 cell. *Cell Struct. Funct.*, 38:21–30.

Kull, F. J., Sablin, E. P., Lau, R., Fletterick, R. J. & Vale, R. D. 1996. Crystal structure of the kinesin motor domain reveals a structural similarity to myosin. *Nature*, 380:550–555.

Kushida, Y., Nakano, K. & Numata, O. 2011. Amitosis requires γ-tubulin-mediated microtubule assembly in *Tetrahymena thermophila*. *Cytoskeleton*, 68:89–96.

Kushida, Y., Takaine, M., Nakano, K., Sugai, T. & Numata, O. 2015. Dynamic change of cellular localization of microtubule-organizing center during conjugation of ciliate *Tetrahymena thermophila*. *Zool. Sci.*, 32:25–32.

LaFountain Jr, J. R. & Davidson, L. A. 1979. An analysis of spindle ultrastructure during prometaphase and metaphase of micronuclear division in *Tetrahymena*. *Chromosoma*, 75:293–308.

LaFountain Jr, J. R. & Davidson, L. A. 1980. An analysis of spindle ultrastructure during anaphase of micronuclear division in *Tetrahymena*. *Cell Motil.*, 1:41–61.

Lee, S., Wisniewski, J. C., Dentler, W. L. & Asai, D. J. 1999. Gene knockouts reveal separate functions for two cytoplasmic dyneins in *Tetrahymena thermophila*. *Mol. Biol. Cell*, 10:771–784.

Loidl, J., Lukaszewicz, A., Howard-Till, R. A. & Koestler, T. 2012. The *Tetrahymena* meiotic chromosome bouquet is organized by centromeres and promotes interhomolog recombination. *J. Cell Sci.*, 125:5873–5880.

Loidl, J. & Mochizuki, K. 2009. *Tetrahymena* meiotic nuclear reorganization is induced by a checkpoint kinase-dependent response to DNA damage. *Mol. Biol. Cell*, 20:2428–2437.

Loidl, J. & Scherthan, H. 2004. Organization and pairing of meiotic chromosomes in the ciliate *Tetrahymena thermophila*. *J. Cell Sci.*, 117:5791–5801.

Martindale, D. W., Allis, C. D. & Bruns, P. J. 1982. Conjugation in *Tetrahymena thermophila*. A temporal analysis of cytological stages. *Exp. Cell Res.*, 140:227–236.

McDonald, H. B., Stewart, R. J. & Goldstein, L. S. 1990. The kinesin-like ncd protein of *Drosophila* is a minus end-directed microtubule motor. *Cell*, 63:1159–1165.

Mochizuki, K., Novatchkova, M. & Loidl, J. 2008. DNA double-strand breaks, but not crossovers, are required for the reorganization of meiotic nuclei in *Tetrahymena*. *J. Cell Sci.*, 121:2148–2158.

Mountain, V., Simerly, C., Howard, L., Ando, A., Schatten, G. & Compton, D. A. 1999. The kinesin-related protein, HSET, opposes the activity of Eg5 and cross-links microtubules in the mammalian mitotic spindle. *J. Cell Biol.*, 147:351–366.

Nanney, D. L. 1964. Macronuclear differentiation and subnuclear assortment in ciliates. *In:* Locke, M. (ed.), The Role of Chromosomes in Development. Academic Press, New York, NY. p. 253–273.

Orias, E. & Flacks, M. 1975. Macronuclear genetics of *Tetrahymena*. I. Random distribution of macronuclear genecopies in *T. pyriformis*, syngen 1. *Genetics*, 79:187–206.

Orias, J. D., Hamilton, E. P. & Orias, E. 1983. A microtubule meshwork associated with gametic pronucleus transfer across a cell-cell junction. *Science*, 222:181–184.

Pechatnikova, E. & Taylor, E. W. 1997. Kinetic mechanism of monomeric non-claret disjunctional protein (Ncd) ATPase. *J. Biol. Chem.*, 272:30735–30740.

Pechatnikova, E. & Taylor, E. W. 1999. Kinetics processivity and the direction of motion of Ncd. *Biophys. J.*, 77:1003–1016.

Raikov, I. B. 1982. The protozoan nucleus. Springer-Verlag Wien, New York, NY. p 253.

Ray Jr, C. 1956. Meiosis and nuclear behavior in *Tetrahymena pyriformis*. *J. Protozool.*, 3:88–96.

Sablin, E. P., Kull, F. J., Cooke, R., Vale, R. D. & Fletterick, R. J. 1996. Crystal structure of the motor domain of the kinesin-related motor ncd. *Nature*, 380:555–559.

Schmit, A. C., Vantard, M., de Mey, J. & Lambert, A. M. 1983. Aster-like microtubule centers establish spindle polarity during interphase – mitosis transition in higher plant cells. *Plant Cell Rep.*, 2:285–288.

Schuh, M. & Ellenberg, J. 2007. Self-organization of MTOCs replaces centrosome function during acentrosomal spindle assembly in live mouse oocytes. *Cell*, 130:484–498.

Shang, Y., Song, X., Bowen, J., Corstanje, R., Gao, Y., Gaertig, J. & Gorovsky, M. A. 2002. A robust inducible-repressible promoter greatly facilitates gene knockouts, conditional expression, and overexpression of homologous and heterologous genes in *Tetrahymena thermophila*. *Proc. Natl Acad. Sci. USA*, 99:3734–3739.

Sharp, D. J., Yu, K. R., Sisson, J. C., Sullivan, W. & Scholey, J. M. 1999. Antagonistic microtubule-sliding motors position mitotic centrosomes in *Drosophila* early embryos. *Nat. Cell Biol.*, 1:51–54.

Stevenson, I. 1972. Ultrastructure of nuclear division in *Paramecium aurelia*. III. Meiosis in the micronucleus during conjugation. *Aust. J. Biol. Sci.*, 25:775–799.

Sugai, T. & Hiwatashi, K. 1974. Cytologic and autoradiographic studies of the micronucleus at meiotic prophase in *Tetrahymena pyriformis*. *J. Protozool.*, 21:542–548.

Suganuma, Y. & Yamamoto, H. 1992. Conjugation in *Tetrahymena*: ultrastructure of the meiotic prophase of the micronucleus. *Eur. J. Protistol.*, 28:434–441.

Tamura, S., Tsuruhara, T. & Watanabe, Y. 1969. Function of nuclear microtubules in macronuclear division of *Tetrahymena pyriformis*. *Exp. Cell Res.*, 55:351–358.

Tao, L., Mogilner, A., Civelekoglu-Scholey, G., Wollman, R., Evans, J., Stahlberg, H. & Scholey, J. M. 2006. A homotetrameric kinesin-5, KLP61F, bundles microtubules and antagonizes Ncd in motility assays. *Curr. Biol.*, 16:2293–2302.

Theurkauf, W. E. & Hawley, R. S. 1992. Meiotic spindle assembly in *Drosophila* females: behavior of nonexchange chromosomes and the effects of mutations in the nod kinesin-like protein. *J. Cell Biol.*, 116:1167–1180.

Wasteneys, G. O. 2002. Microtubule organization in the green kingdom: chaos or self-order? *J. Cell Sci.*, 115:1345–1354.

Wickstead, B., Gull, K. & Richards, T. A. 2010. Patterns of kinesin evolution reveal a complex ancestral eukaryote with a multifunctional cytoskeleton. *BMC Evol. Biol.*, 10:110. doi:10.1186/1471-2148-10-110.

Williams, N. E. & Williams, R. J. 1976. Macronuclear division with and without microtubules in *Tetrahymena*. *J. Cell Sci.*, 20:61–77.

Winey, M. & Bloom, K. 2012. Mitotic spindle form and function. *Genetics*, 190:1197–1224.

Wolfe, J., Hunter, B. & Adair, W. S. 1976. A cytological study of micronuclear elongation during conjugation in *Tetrahymena*. *Chromosoma*, 55:289–308.

Wunderlich, F. & Peyk, D. 1969. Antimitotic agents and macronuclear division of ciliates. I. Colchicine and colcemid in exponentially growing cultures of *Tetrahymena pyriformis* GL. *Naturwissenschaften*, 56:285–286.

Wunderlich, F. & Speth, V. 1970. Antimitotic agents and macronuclear division of ciliates. IV. Reassembly of microtubules in macronuclei of *Tetrahymena* adapting to colchicine. *Protoplasma*, 70:139–152.

Xiong, J., Lu, Y., Feng, J., Yuan, D., Tian, M., Chang, Y., Fu, C., Wang, G., Zeng, H. & Miao, W. 2013. *Tetrahymena* functional genomics database (TetraFGD): an integrated resource for *Tetrahymena* functional genomics. *Database* (Oxford University Press), 2013:bat008. doi: 10.1093/database/bat008.

SUPPORTING INFORMATION

Additional Supporting Information may be found online in the supporting information tab for this article:

Figure S1. Strategies for double gene KO of *KIN141* and *KIN142*.

Figure S2. The frequency distribution of the phenotype of *KIN141*-KO × *KIN141*-KO crosses during conjugation.